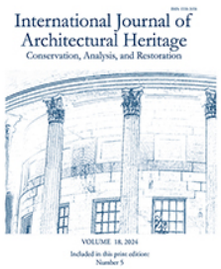

International Journal of Architectural Heritage
Conservation, Analysis, and Restoration

ISSN: (Print) (Online) Journal homepage: www.tandfonline.com/journals/uarc20

Graphic Statics for Continuous Beams and Frames: A Review of the Fixed-points Method

Shuyuan Han & Denis Zastavni

To cite this article: Shuyuan Han & Denis Zastavni (10 May 2024): Graphic Statics for Continuous Beams and Frames: A Review of the Fixed-points Method, International Journal of Architectural Heritage, DOI: 10.1080/15583058.2024.2352488

To link to this article: https://doi.org/10.1080/15583058.2024.2352488

INTERNATIONAL JOURNAL OF ARCHITECTURAL HERITAGE
https://doi.org/10.1080/15583058.2024.2352488

Graphic Statics for Continuous Beams and Frames: A Review of the Fixed-points Method

Shuyuan Han and Denis Zastavni

Louvain research institute for Landscape, Architecture, Built environment [LAB], Université catholique de Louvain, Louvain-la-Neuve, Belgium

ABSTRACT

Graphic statics not only applies to statically determinate systems but also extends to indeterminate systems. This paper reviews a historical graphical method tailored for continuous beams and frames: the *fixed-points method*. Despite its current obscurity, the *fixed-points method* played a crucial role in the repertoire of graphic statics and enjoyed considerable popularity during the late 19th and early 20th centuries. Our review outlines its historical evolution, explains its principles and techniques, and illuminates Robert Maillart's applications of this method in the Simme bridge in Garstatt and the Weissensteinstrasse Overpass in Bern.

ARTICLE HISTORY
Received 10 January 2024
Accepted 26 April 2024

KEYWORDS
Continuous beam; continuous frame; graphic statics; Robert Maillart; statically indeterminate system; the fixed-points method

1. Introduction

1.1. Graphic statics

Graphic statics is a classic geometric-based approach for structure analysis and design. It encompasses a variety of graphical methods tailored for different structure types (Allen and Zalewski 2009; Saliklis 2019). This method relies on graphical diagrams rather than algebraic calculations to ascertain the internal forces and reactions of a structure. Graphic statics was extensively studied and applied in the late 19th and early 20th centuries but was almost totally supplanted by algebraic and numerical methods by the mid-20th century.

In recent years, there has been a partial resurgence of graphic statics. Due to its unparalleled visual clarity, graphics statics has been rediscovered as an insightful method for structure, leveraging enhanced efficiency through computerization (D'acunto et al. 2019; Fivet and Zastavni 2015). Additionally, this renewed application of graphic statics into the design was accompanied and inspired by the investigation of historical designs and writings (Huerta 2006; Zastavni 2008). Furthermore, it finds renewed application in the analysis of historical masonry structures (Block and Lachauer 2014; Costa-Jover, Lluis i Ginovart, and Coll-Pla 2017; Cusano et al. 2023; Fang et al. 2019; Karanikoloudis et al. 2021; Kavanaugh et al. 2017; Ramos and Sturm 2014).

1.2. The fixed-points method

Regrettably, contemporary scholarly work on graphic statics tends to focus primarily on statically determinate structural systems. This focus has contributed to the prevailing misconception that graphic statics cannot be applied to statically indeterminate systems. However, graphical methods for the elastic analysis of continuous beams and frames, which fall under the category of statically indeterminate systems, were indeed a significant component of the arsenal of graphic statics. This is unsurprising given that the era when graphic statics was rapidly developed and increasingly applied coincided with the rise of continuous structures. Many monographs on graphic statics then, including some standard ones (Culmann 1866; Ritter and Culmann 1900), endeavored to extend the application of graphic statics to these emerging structure types.

Among these methods, the *fixed-points method* (German: *Methode der Festpunkte*) stands out as the earliest and arguably the most influential one. Ernst Suter, a pivotal figure in the development of this method, remarked, "*Because of its clarity, the fixed-points method is rightly very popular among engineers*" (Suter 1923, V). Besides, this method was regarded as one of the most well-known approaches in practical engineering, as noted by (Guldan 1943, 145). As a case in point, the authors discovered that the renowned Swiss engineer Robert Maillart applied the *fixed-points*

CONTACT Shuyuan Han hanshuyuan91@gmail.com; shuyuan.han@uclouvain.be Louvain research institute for Landscape, Architecture, Built environment [LAB], Université catholique de Louvain, Place du Levant 1 (L5.05.02) - B, Louvain-la-Neuve 1348, Belgium

method in his analysis of two bridges: the Simme bridge in Garstatt and the Weissensteinstrasse Overpass in Bern.

1.3. Relevant researches

Recently, the historical graphical methods tailored for continuous beams and frames have begun to receive limited attention in scholarly works. T. Boothby reviewed Charles Greene's semi-graphical method for continuous girders (Boothby 2015, 198–200). E. Saliklis has provided a lucid and pedagogical explanation of a graphical method which solves continuous beams with funicular polygons (Saliklis 2019, 213–248). A similar method for continuous beams and portal frames was reviewed by the authors (Han, 2022). In addition, before the current resurgence of graphic statics, Charlton reviewed another graphical method named the *characteristic points method* which was invented by Thomas Claxton Fidler (Charlton 1982). While these three methods share some theoretical foundations with the *fixed-points method*, they primarily differ in their approach to solving static indeterminacy. They all employ a tentative approach as opposed to the synthetic approach of the *fixed-points method*.

A comprehensive review dedicated to the *fixed-points method* seems to be absent in contemporary writings to the best of our knowledge. Although a historical drawing employing the *fixed-points method* was included in the monograph of historical engineering methods by T. Boothby, no accompanying explanation was provided (Boothby 2015, 197). Furthermore, this method was only briefly mentioned in the encyclopedic book on the history of structural theory by K. Kurrer, while the evolution of the graphical methods for statically determinate systems was reviewed in detail (Kurrer 2018, 702). The most recent literature detailing the principles and techniques of the *fixed-points method* known to the authors dates back to the late 1960s and is more focused on the numerical version of this method instead of the graphical one (Sattler 1969). The current state of obscurity surrounding this method does not match its historical significance. Keeping this in perspective, the authors have undertaken an initial examination of this method (Han, 2023).

1.4. Research aim, significance, and outline

To this end, this paper aims to present a review of the *fixed-points method*, including its historical evolution, principles, techniques, and application cases.

This review of the *fixed-points method* could potentially contribute to the preservation of historical structures designed using this method. The absence of knowledge regarding this method might impede the accurate interpretation of original design documents, leading to potential pitfalls in preservation design. Take the Weissensteinstrasse Overpass as an example. Although this bridge was originally designed as a continuous frame, it has long been erroneously associated with continuous beams supported by hinged pillar head (Bill 1955, 132; Billington 1979, 125). Its maximum load capacity will be underestimated if it is preserved as a continuous beam. Considering the purported popularity of this method, such a review could inform numerous preservation designs.

Additionally, the *fixed-points method* constitutes a significant aspect of intangible architectural cultural heritage, sharing equal importance of the cultural value with historical structures to which it was applied. In the field of cognition and teaching, the recent resurgence of graphic statics as an insightful design tool has illustrated the special merits of graphical methods that were once considered obsolete (Hartz et al. 2018). *The fixed-points method* also exhibits superiority over prevailing contemporary methods in visualizing the relation between member stiffness and bending moment.

The remaining sections of this study are organized as follows: Section 2 outlines the evolution of this method, which is periodized according to its historical context of construction. Section 3 delves into the theoretical foundations of the method. Sections 4 elucidates the rationale of the fixed points, which serves as the core technique for solving static indeterminacy. The procedures for analyzing continuous beams and frames are explained in Sections 5 and 6, respectively. Section 7 sheds light on Robert Maillart's application of this method in two bridges. Finally, Section 8 summarizes the main points, highlights contributions, and discusses potential avenues for future research.

2. The evolution of the fixed-points method

The fixed-points method was invented by Christian Otto Mohr (1835–1918) in 1868 in his seminal work "*Beiträge zur Theorie der Holz- und Eisenkonstruktionen*" (*Contribution to the Theory of Wood and Iron Constructions*) (Mohr 1868). It underwent successive developments by various engineers before becoming obsolete in the second half of the 20th century. According to the different theoretical interest generated by construction practices, the evolution of this method can be broadly periodized into (Figure 1):

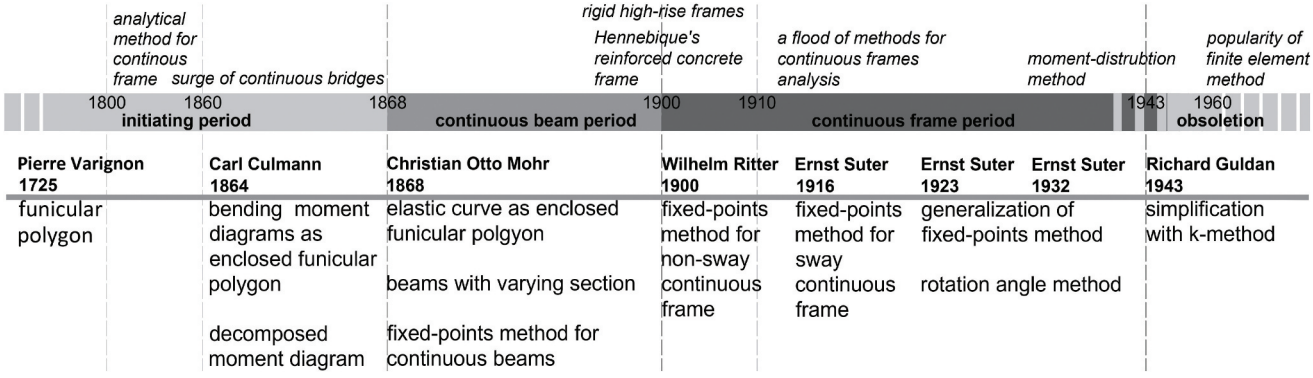

Figure 1. The evolution of the *fixed-points method*.

(1) The era of continuous beams (from 1868 to around 1900).
(2) The era of continuous frames (about the first half of the 20th century).

2.1. In the era of continuous beams (from 1868 to around 1900)

2.1.1. The proliferation of continuous bridges

The mid-19th century witnessed a notable surge of continuous-beam bridges driven by railway expansion and the increased use of wrought iron. The continuous beam often exhibits greater structural efficiency compared to consecutive simply supported beams, as the continuous joints reduced the maximum moment at the mid-span. This structural efficiency proved beneficial, especially in designing railway bridges where high bearing capacities were crucial. Additionally, during this period, the transition from cast iron to wrought iron effectively addressed the challenge of creating continuous joints. Wrought iron has balanced tensile and compressive strength and is ductile enough for riveting. These favorable properties facilitated the construction of continuous connections, further driving the adoption of this efficient structural type.

However, the high cost of wrought iron demanded a more precise engineering of continuous beams for economic viability. Additionally, the statically indeterminate nature of continuous beams presented an analytical challenge. As the number of supports exceeded two, the internal forces couldn't be determined solely by static equations.

Consequently, the structural analysis of continuous beams became a focal point in engineering research, leading to the development of various analysis methods tailored for this structure type. Before this, the foundation stones of the algebraic method for continuous beams were laid successively by Johann Albert Eytelwein and Claude-Louis Navier in the early 19th century. Émile Clapeyron's publication of the theorem of three moments in 1857 furthered this development. The emerging theories swiftly found application in construction projects like the Britannia Bridges (constructed in 1846–50), showcasing unprecedented scales of continuous beams. These algebraical methods have been extensively reviewed by (Charlton 1982; Kurrer 2018).

2.1.2. The theoretical groundwork for the fixed-points method

The era of the proliferation of continuous beams coincided with the establishment of graphic statics, notably marked by Carl Culmann's (1821–1881) landmark book *Die graphische Statik* (*the Graphic Statics*) (Culmann 1866). As an experienced engineer of iron bridges, Carl Culmann sought to extend this new discipline to the analysis of continuous beams. His book extensively discussed the analysis of continuous beams, dedicating an entire section to this topic (Culmann 1866, 273–351). However, Culmann encountered difficulties in developing a graphical method for continuous beams due to the challenge of analyzing deflection graphically—an essential aspect in analyzing statically indeterminate structures. Culmann's attempts were hindered by the complexity of his curvature formula, which proved too intricate for graphical representation (Culmann 1866, 289).[1] Consequently, he then settled for a somewhat abstruse algebraical approach.

Nonetheless, Culmann laid the foundational groundwork for graphical methods in analyzing beam bending through his method for constructing bending moment

[1]The modern formula for curvature, which is simplified yet sufficiently precise, had already been discovered decades ago of by (Navier 1833, 49) and (Rankine and Roberts 1858, 160–161). However, these findings were regrettably unknown unto Culmann.

diagrams of statically determinate beams. He found that the bending moment diagram of plane beams could be analogously constructed as an enclosed funicular polygon (Culmann 1866, 124–132). Moreover, Culmann highlighted that the bending moment diagram of continuous beams could be depicted by the overlapping diagrams of statically determinate and indeterminate moments (Culmann 1866, 274).

Culmann's method was built upon Pierre Varignon's (1645–1722) graphical method for constructing the funicular polygon, which represents the equilibrium position of an inelastic suspended rope under loads (Varignon 1725). Varignon's method was based on the law of the parallelogram of forces, a principle progressively revealed by Leonardo da Vinci, Simon Stevin, Gilles de Roberval, and Isaac Newton (Capecchi 2012).

Another pivotal advancement for the invention of the *fixed-points method* was achieved by Christian Otto Mohr (1835–1918) in the same paper which presented this method (Mohr 1868). With the simplified formula for curvature, Mohr revealed that the elastic curve of a beam could also be represented as an enclosed funicular polygon by analogically taking moment area as the 'loading'.

Varignon, Culmann and Mohr's contribution will be explained in *section 3*.

2.1.3. The invention and dissemination of fixed-points method for continuous beams

With the foundation work of Varignon and Culmann and his method for elastic curves, Mohr invented *the fixed-points method* (Mohr 1868). This method derived its name from its unique approach to addressing static indeterminacy through geometric constraints of fixed points on the bending moment diagram. Mohr located these fixed points using specific elastic curves, which are referred to as *abstract elastic curves* in this paper. Additionally, he introduced the technique of *crossing lines* (*kreuzlinien*) to ascertain the bending moment of loaded spans. Furthermore, Mohr expanded the method to accommodate continuous beams with varying second moments of area.

Mohr's groundbreaking work prompted responses from Culmann and Karl Wilhelm Ritter (1847–1906). Ritter was Culmann' pupil and was then working as Culmann's assistant and a privatdozent at ETH Zürich. With Culmann's consent, Ritter published a concise book to introduce Mohr's elastic curve and *fixed-points method* to the Culmann's audience (Ritter 1871), which was revised and reprinted in was 1883 (Ritter 1883). In this book, Ritter confined the application to simpler cases involving continuous beams with a constant cross-section and a uniformly distributed load, which he believed would suffice in most practical scenarios.

Culmann also incorporated Mohr's funicular of elastic curve for analyzing one-span statically indeterminate beams, in the first volume of the expanded second edition of *Die graphische Statik* (Culmann 1875, 627–644, Pl. 617). He promised to dedicate a section in the subsequent volume specifically to the systematic use of the *fixed-points method* for analyzing continuous beams (Culmann 1875, 627). Unfortunately, he passed away before completing the second volume.

Subsequently, Ritter published the long-awaited monograph on the analysis of continuous beams as the third volume of his series "*Anwendungen der graphischen Statik*" (*Applications of Graphic Statics*) in 1900 (Ritter and Culmann 1900). Ritter took over Culmann's unfinished research on graphic statics and professorship in 1882. However, rather than continuing Culmann's work, Ritter initiated his comprehensive series on graphic statics and postponed writing about the analysis of continuous frames. Furthermore, delays in this monograph resulted from Ritter's extensive engagements in bridge engineering practice (Ritter and Culmann 1900, IV).

This monograph represented the pinnacle of applying the *fixed-points method* to continuous beams. In the preface, Ritter acknowledged Mohr's significant contributions, remarked that,

> Rarely has such a simple idea yielded such rich fruits as Mohr's method for drawing the elastic curve. Since then, stone after stone has been added to the foundation laid at that time, and today we have come to the point where we can not only answer the most mundane questions belonging here with playful ease, but also hardly flinch from the most difficult tasks presented to us by civil engineering. (Ritter and Culmann 1900, V)

Ritter showcased various problem-solving applications of the *fixed-points method* in analyzing continuous beams, including trussed continuous beams with varying height. He highlighted the simplicity and clarity of this graphical method in solving tasks compared to algebraic methods.

Beyond Switzerland, the renowned German professor Heinrich Müller-Breslau included the *fixed-points method* in his influential book (Müller-Breslau 1892, 352–356). However, his approach focused more on analytical formulas rather than graphical drawing in determining fixed points and moments.

In non-German-speaking countries, along with the translation of Ritter's works, the *fixed-points method* was introduced by various engineers. It was introduced to America by Augustus Jay Du Bois (Du Bois 1875), and later to Britain by James Chalmers (Chalmers 1881).

In France, Maurice Lévy incorporated the *fixed-points method* into the expanded second version of his influential monograph on graphic statics (Levy 1886, 321–343). Maurice Koechlin, a student of Culmann known for his pivotal contribution to the Eiffel Tower, included this method in his book (Koechlin 1889, 345–361). Additionally, the method found a place in (Pillet 1895, 218–250), which was developed from the Pillet's teaching.

2.2. The era of continuous frames (around the first half of the 20th century)

Ritter's monograph also marked the shift in the interest of theoretical exploration, transitioning from continuous beams to continuous frames. On one hand, Ritter noted a declining preference among engineers for continuous bridges as the drawbacks of this structural type were scrutinized more thoroughly (Ritter and Culmann 1900, IV). On the other hand, Ritter extended the *fixed-points method* to continuous frame bridges without lateral displacement (Ritter and Culmann 1900, 125–146).

2.2.1. The widespread use of continuous frames and early algebraical methods

The transition towards analyzing continuous frames was influenced by the proliferation of this system in construction practices. During the 19th century, continuous frames remained a relatively uncommon structural type. However, in the early 20th century their prevalence was notably increasing with the emergence of skyscrapers and the expanding use of materials like steel and, notably, reinforced concrete. Due to the magnitude of wind load and the slender profile of skyscrapers, the issue of lateral bracing became a central concern. The continuous frame was utilized as a spatially efficient and flexible solution for lateral bracing, as it is free from diagonal bracings which could impede inner space or envelope opening. Concurrently, the French engineer and entrepreneur François Hennebique pioneered the first monolithic reinforced concrete frame, integrating all structural elements into a continuous system. Hennebique's commercial success inspired the proliferation of patented monolithic reinforced concrete structures from the mid-1890s to the mid-1910s. These frame systems, including Hennebique's, often derived lateral stability from their continuous beam-column joints.

However, the analytical methods initially devised for continuous beams were often impractical for continuous frames due to distinct challenges. First, continuous frames generally possess a higher degree of static indeterminacy. Solving a statically indeterminate system using analytical methods requires solving an equation system with as many equations as the degree of indeterminacy. In an era of manual calculation, even a system of merely six equations would challenge most engineers. Consequently, engineers often resorted to approximation methods like the portal method and cantilever method, although their precision was often unreliable (Kurrer 2018, 818). Second, continuous frames are often used to withstand lateral loads applied at beam-column joints rather than on members. This application cannot be addressed by the theory for continuous beams.

2.2.2. The extension of the fixed-points method to continuous frames

It is in this context that the *fixed-points method* evolved from a technique tailored for continuous beams to a method centered on continuous frames.

Ritter made the first step by considering single-story continuous frames as exceptional cases of continuous beams. He modified the method for locating fixed points by incorporating column moment resistance. Additionally, Ritter introduced the *moment distribution angle* to graphically distribute bending moment at continuous joints.

This transition was significantly advanced by the Swiss engineer Ernst Suter (1884–1929). Suter's doctoral dissertation extended the *fixed-points method* to analyze frames with horizontal displacement, contextualizing his theory within the realm of reinforced concrete frames (Suter 1916). Notably, his research specialized in analyzing frames with varying member section lengths, enabled by the adaptability of reinforced concrete to diverse forms.

After his dissertation, Suter continued his research to generalize the *fixed-points method*. He extensively applied and refined this methodology in his role of chief engineer at the prominent reinforced concrete construction company Wayss & Freytag AG. Suter's research and practice were crystalized into the book titled as the *fixed-points method* (Suter 1923). Due to his expertise, he obtained the position of privatdozent at ETH Zürich, where he taught the *fixed-points method* between 1924 and 1927 (ETH-Archiv 2018). Unfortunately, Suter's untimely demise in 1929 interrupted his contributions, leading to the posthumous completion of an updated version by two of his office associates (Suter, Baumann, and Häusler 1932), adhering to his original intent.

At this stage, the *fixed-points method* had evolved to encompass the analysis of nearly all encountered statically indeterminate frames in practical scenarios. Its

versatility extended to multiple-span and multi-story continuous frames, accommodating complex loading, arbitrarily oriented bars, arched structures, and addressing various types of loading. Furthermore, it was adept at analyzing stress induced by thermal changes and foundation settlements. The capability of graphical methods to handle complex issues reached an unprecedented pinnacle.

In addition to the graphical method, Suter developed the algebraical version of the *fixed-points method*, known as the *rotation angle method* (*der Drehwinkelmethode*). This method is based on numerous rotation angles calculated for each member and joint under an imaginary unit moment (Suter 1923, 19–22). These angles represent the stiffness of all the members and joints from various perspectives. The fixed points and crossing lines can be derived from these rotational angles. While the graphical analysis involves a substantial amount of drawing due to the complexity of the problem, the algebraical approach of the *fixed-points method* serves as a potential shortcut. Therefore, the *fixed-points method* evolved into a fusion of two parallel approaches: graphical and algebraical. The analysis can be conducted partly through graphs and partly through calculations, mutually corroborating each other. However, due to space constraints, the algebraical approach will not be expounded upon in this paper.

2.2.3. The attempt of simplifying the fixed-points method

Suter's method gained prominence within the German-speaking region, where there was a strong tradition of Culmann's graphical method. However, outside this region, the influence of the *fixed-points method* seemed to wane. The 20th century's English writing on introducing the *fixed-points method* to English readers that the authors have found was (Robin 1933). Furthermore, with the emergence of Cross Hardy's *moment distribution method* (Cross 1932), the *fixed-points method* faced competition from the rapidly spreading numerical techniques.

The disadvantage of the *fixed-points method*, particularly against the *moment distribution method*, can be primarily attributed to its complexity. Even in its less sophisticated application to continuous beams, *the fixed-points method* was considered "*challenging to understand*" by (Boothby 2015, 197). Suter's quest for a comprehensive solution to continuous frames, while admirable, escalated the complexity. For instance, the *rotation angle method* is based on 12 types of angles (Suter, Baumann, and Häusler 1932, 18–20). Besides, Suter's extension for frames with varying section within spans didn't align well with the prevalent practical use of reinforced concrete frames where constant sections within spans were more common. In comparison, the *moment distribution method* is relatively easier to comprehend and is tailored to frames with inertia varying span-wise.

To streamline Suter's legacy and align it more closely with practical needs, Richard Guldan (1901–1955), a Sudeten German Professor, introduced a algebraical method: *the k-method* (*k-verfahren*) (Guldan 1943, 154–167). Unlike the somewhat intricate *rotation angle method*, *the k-method* was tailored for frames whose second area moment only varied span-wise. In this method, the stiffness of a member is represented as "*k*", equivalent to its moment of inertia divided by its length. The parameter *k* indicates the rotational stiffness, given all the members are in the same material. The location of fixed points and crossing lines are analytically derived from the stiffness *k*. Guldan's work led to the third edition of the book *fixed-points method* by Ernst Traub (Henn 1951), which focused on the *k-method*. This method also found its place in the classic textbook of statics by (Hirschfeld 1959; Sattler 1969).

However, the *fixed-points method* for indeterminate structures faded into obscurity with the rise of the *finite element method* in the 1960s. The *finite element method*, more compatible with early computers, became dominant in practice, aided by rapidly advancing computer technology.

3. The theoretical foundation of fixed-points method

3.1. The graphical method for funicular polygon

Pierre Varignon found that the funicular polygon of a loaded rope can be graphically constructed through a *force diagram*. For instance, in Figure 2 the funicular polygon of *ABCDEF*, which resulted from the given loads f_1 – f_4, is determined using the force polygon on the right. Besides, the resultant of all the loads must pass through point *G*, which is the intersection of the extension of edges *AB* and *FE*. For a more detailed explanation, refer to (Allen and Zalewski 2009, 37–43; Saliklis 2019, 31–56).

3.2. The analogy between enclosed funicular polygon and the bending action of beams

Carl Culmann found that by incorporating a closing string, the funicular polygon could ascertain the bending moment and reactions of a beam. Consider the simply supported beam *A'F'* depicted in Figure 2. This beam and

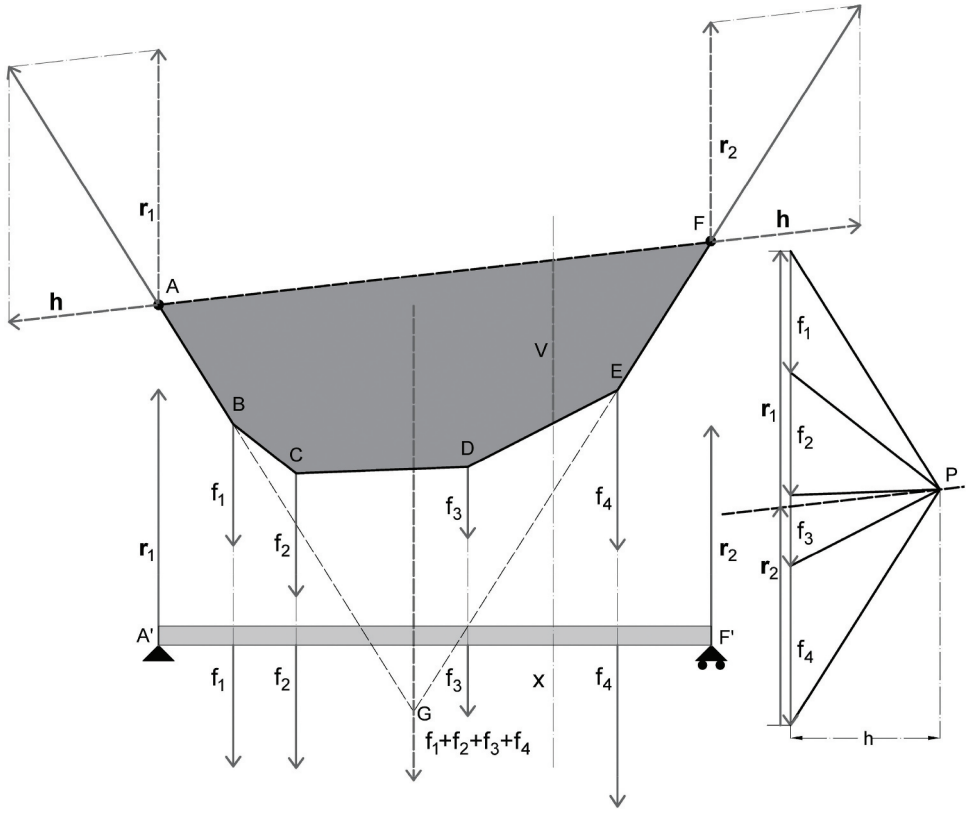

Figure 2. The funicular polygon (left), its corresponding force polygon (right), and a simply supported beam under same loads (bottom).

the above funicular polygon possess equal spans and are under identical loads. Connecting the ends of the funicular polygon with the closing string *AF* generates the enclosed polygon, representing the bending moment of the beam. The skewed reference line is denoted by *AF*. The scale of this bending moment diagram is the multiplicative inverse of the pole distance *h* in the *force diagram*. In simpler terms, the bending moment at an arbitrary vertical line *x* equals *h* multiplied by *v*, in which *v* signifies the corresponding vertical distance between the funicular polygon and the closing string.

Moreover, the magnitude of vertical reactions R_1 and R_2 at the supports can be readily determined by drawing a parallel line of the closing string *AF* through the pole *P*. This parallel line divides the vertical of the *force diagram* into two parts, each representing a support reaction. The detailed demonstration can be referenced in (Allen and Zalewski 2009, 437–442) and (Saliklis 2019, 57–70).[2]

Otto Mohr revealed that the elastic curve of a beam could also be represented as an enclosed funicular polygon by analogically taking moment area as the "force" and bending stiffness *(EI)* as the pole distance as the "*force diagram*" (Mohr 1868). The "force" is figuratively termed as "*elastic weight*" (*elastisches Gewicht*) by (Suter 1916, 13), and the special "*force diagram*" will be referred to as *MΔx polygon/diagram*[3] as the load force is replaced by the discretized moment area ($M^*\Delta x$). The pole distance (*EI*) in the elastic curve representation is typically scaled down by a factor of *n* for ease of graphical depiction. Consequently, the deflection is scaled up by a factor of *n*. The demonstration can be found in (Saliklis 2019, 213–248).

For example, in Figure 3, the bending moment diagram of the beam is sliced into reasonably short segments (the pole distance of force diagram is set equal to one). The moment areas of the segments are considered as an array of elastic weights, which are applied at the centroids of the respective moment areas. The construction of the funicular polygon for the elastic curve involves using the *MΔx diagram*, where the pole distance is *EI/n*. Consequently, the vertical distance

[2]It is worth noting that this analogy can be readily extended to beams with inclined loadings (Wolfe 1921, 26) and moment-resisting three-hinge arches (Saliklis 2019, 70–77).

[3]In Mohr's original paper, this diagram was referred to simply as the *'auxiliary figure' (Hülfsfigur)* (Mohr 1868). The naming *'MΔx force polygon'* closely follows the designation provided by (Chalmers 1881, 200), which was one of the earliest introductions of Mohr's method to English readers. Chalmers termed this diagram the '*MΔy force polygon*', utilizing '*y*' as the designation for the beam length dimension.

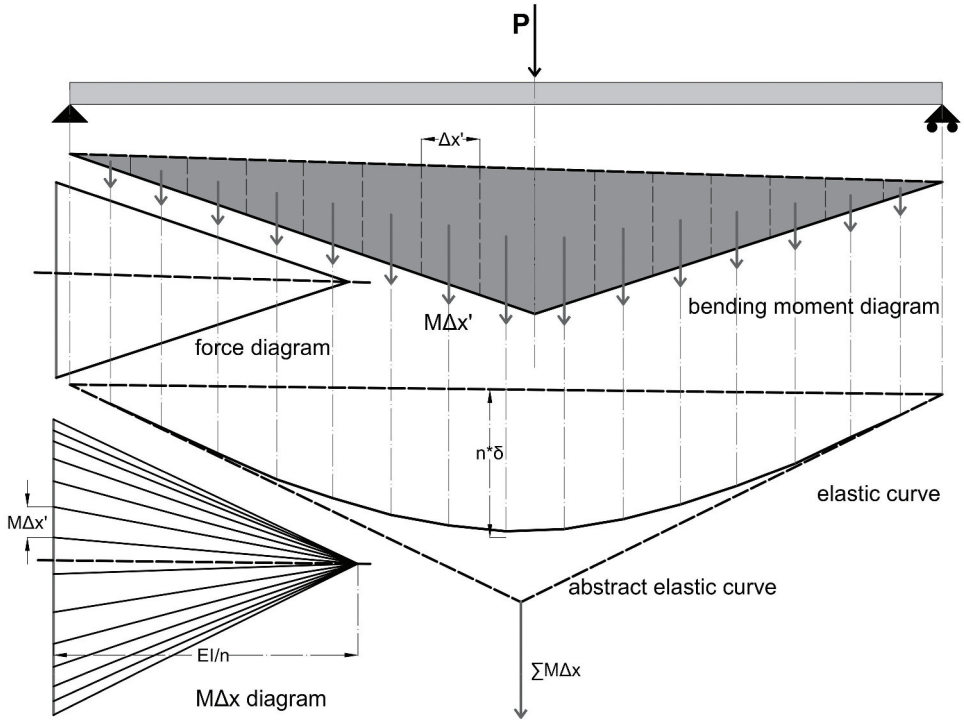

Figure 3. The graphical method of determining the elastic curve of a simply supported beam.

between the funicular polygon of elastic curve and the closing string equates to n times the actual deflection δ.

It is important to note that the quantity of moment segments does not affect the slope of the ends of funicular polygon. As a result, the difference in slope between the two supports can be more easily determined using the *abstract elastic curve* (represented by dashed lines), loaded by the cumulative moment area ($\sum M\Delta x$) of the bending moment diagram.

Today, Mohr's finding is better known in its algebraic version: the moment-area theorem or Mohr's theorem. Compared to the algebraic version, the graphical approach provides greater visual clarity, particularly in depicting the relationship between bending stiffness and deflection. This graphical method proves advantageous, especially for beams with varying sections, as showcased in examples detailed in (Wolfe 1921, 94–95).[4]

3.3. The decomposed bending moment diagram of the continuous beam

In the *fixed-points method*, the bending moment diagram serves as a graphical tool for analysis. Upon completion of this diagram, one can deduce shears, support reactions, and deflections. In contrast, the conventional bending moment diagram represents a simplified graph of the abscissa-moment function, displaying the calculated results.

The bending behavior of a continuous beam differs from that of simply supported beams due to the presence of the "joining" moment at the continuous joint. Consequently, the bending moment within a continuous beam can be divided into the moment of load and the "joining" bending moment from the continuous joint (see Figure 4). The moment of load is dictated by the magnitude and distribution of load, and is independent of member stiffness, making it statically determinate. Conversely, the "joining" moment depends on the stiffness of the joined members and is statically indeterminate. Notably, unlike the bending moment diagram of simply supported beams (Figures 2 and 3), the endpoints of the closing strings of a hyperstatic beam do not coincide with those of the funicular polygon. This is because of the presence of the "joining" moment, whose magnitude is represented by the vertical distance between the ends of the funicular polygon and the closing string of hyperstatic beams.

This distinction leads to the bending moment diagram of a continuous beam being depicted as a superposition of funicular polygons and closing strings. The funicular polygon represents the moment of load, while the closing

[4]It is worth noting that Mohr's findings cannot be directly applied to structural members with non-rectilinear axis or under inclined loading. This is because secondary moments may occur in such cases, which can affect deflection.

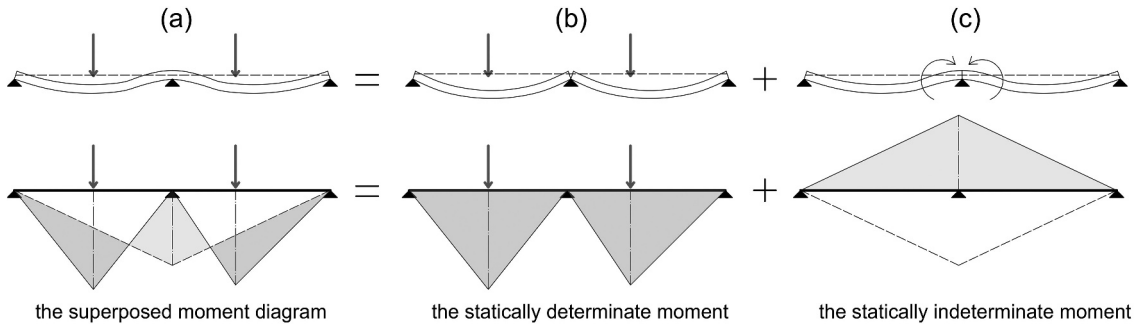

Figure 4. The bending moment diagram of a two-span continuous beam (a) is composed of two superposed parts(b)(c), following the composition of bending moment.

string illustrates bending moment resulted from the "joining" moment. The funicular polygon can be employed to plot the diagram of the moment of load, simplifying the determination of moment within continuous structures to locate the closing string.

Despite their opposite signs, both types of moments are plotted on the same side of the baseline for visual clarity, as demonstrated in Figure 4a. Consequently, the combined moment can be measured by the vertical distance between the funicular and the closing string. The contraflexure points are identified by their intersections.

4. The principles and determination of the fixed points

In the *fixed-points method*, all the statically indeterminacy is resolved by identifying the fixed points within the bending moment diagram.

4.1. The fixity of contraflexure points

The principle underlying fixed points lies in the stationary contraflexure points on the moment diagram of unloaded spans. Put simply, the x-coordinates of the zero-moment points in the unloaded spans remain unchanged despite the loading applied to other spans. For instance, consider the continuous beam illustrated in Figure 5: the contraflexure points in the three right spans maintain their positions irrespective of the loading in the left span. Furthermore, each span has two fixed points. As the moment propagates towards the left, the fixed points on the left part of each unloaded span emerge. If an intermediate span is loaded, then the left fixed points on the left unloaded spans and right fixed points on the right unloaded spans emerge.

The stationarity of contraflexure points is evident due to the linear behavior of elastic structures. When

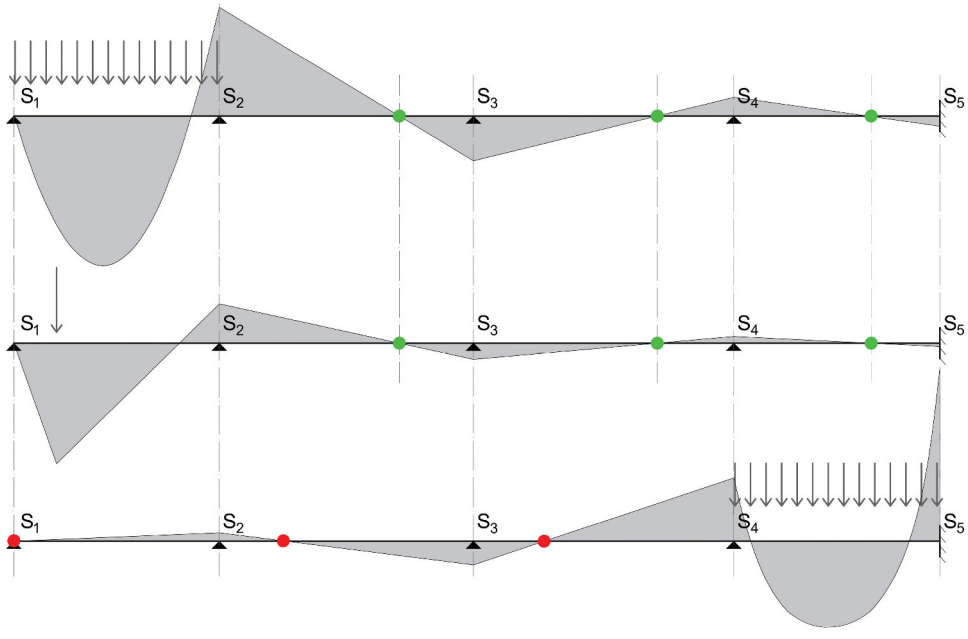

Figure 5. The fixed points of a four-span continuous beam under different loadings.

the spreading moment increases by a factor of 'n', the moment at the contraflexure points also multiplies by 'n', consequently remaining at zero.

The x-coordinates of the fixed points are intrinsic values specific to each span and hinge on the rotational stiffness[5] (EI/L) of that span and the subsequent span relaying the moment. For instance, consider span S_3S_4 in Figure 5: the abscissa of its right fixed point of moment contraflexure is determined by its rotational stiffness and that of span S_4S_5.

In an end span that is fixed at one end — such as span S_4S_5—the fixed point near the clamped end is positioned at the right trisection point. Conversely, in a span hinged at one end, the fixed point near the hinge coincides with the hinge itself. As these points remain zero moment regardless of the moment propagated from other spans.

4.2. The abstract elastic curve of triangulated moment area

The fixed points can be graphically located using the *abstract elastic curve*. Essentially, locating the fixed points is a graphical approach of solving static indeterminacy, thus it must involve analyzing deflection. However, the graphical elastic curve in *subsection 3.2* is quite laborious for solving static indeterminacy due to its numerous moment area segments. We can, however, reduce the workload by minimizing the number of moment area segments. This is because the angular deflection at continuous joints, rather than the linear deflection within the spans, is our primary concern when solving the indeterminacy. And as explained in *subsection 3.2*, the number of moment area segments does not affect the end slope of the funicular polygon.

The *abstract elastic curve* uses triangulated moment areas to minimize the number of moment segments and to fix the action lines of the elastic weights. Consider span AB (length L_1 and stiffness EI) in Figure 6 as an example. It is an unloaded span of a continuous beam and subjected to a leftward-propagated moment. The values of its end moments M_a and M_b are given. To construct its *abstract elastic curve*, the moment area of $AA'B'B$ is divided into overlapping $\Delta AA'B$ and $\Delta BB'A'$. Since the centroid of a triangle divides medians at a ratio of 2:1, the action lines (verticals TT' and UU') of the triangulated elastic weights trisect the span, regardless of M_a and M_b. Hence, these verticals are referred to as "*the trisection line*" (*drittellinien*).

With the fixed action lines, the *abstract elastic curve* A_0TUB_0, representing the funicular polygon formed under the elastic weights of $\Delta AA'B$ and $\Delta BB'A'$, is constructed with the *M*Δ*x diagram*. Since the heights (M_a and M_b) and width (span L_1) of the two triangles are given, the elastic weights, respectively, equal $\frac{M_aL_1}{2}$ and $\frac{M_bL_1}{2}$. Following the signs of M_a and M_b, those of the elastic weights are opposite.

The x-intercept of the *abstract elastic curve* in Figure 6 coincides with the fixed points, which is the zero-moment point (F_1). According to Mohr's Second Theorem (Mohr 1868),[6] the ratio between the lengths of A_0A'' and B_0B'', which denote the y-intercepts of the TU, equates to the ratio between the moment areas of $\Delta AA'B$ and $\Delta BB'A'$. Since the width of both triangles is L_1, this ratio equals the ratio between M_a and M_b, which is expressed as $A_0A : B_0B = M_a : M_b$. It follows that the moment at the intersection between line TU and the baseline must equal zero. This means that the x-intercept of the *abstract elastic curve* (F_1') coincides with the fixed point (F_1) regardless of the magnitude of M_a and M_b. Their shared location depends solely on the ratio between M_a and M_b.

4.3. The abstract elastic curve of continuous spans and the combined trisection line

Without knowledge of the magnitude of bending moment M_b or M_c, we can proceed to construct the *abstract elastic curve* for the unloaded continuous span BC. Assume that the length of BC is L_2 and its bending stiffness is the same as span AB (for spans with different stiffness please refer to *4.4*). Similarly, the moment area of span BC in Figure 6 is dissected into $\Delta BB'C'$ and $\Delta BCC'$, whose centroids V' and X' are fixed on the *trisection lines* VV' and XX'. Extend line UB_0 until it intersects *trisection line* VV' at V. Line B_0V represents the first edge of the *abstract elastic curve*, maintaining the continuity of angular deflection over support B.

The second edge is plotted by utilizing the action line (w) of the resultant of the elastic weights of $\Delta A'B'B$ and $\Delta BB'C'$. The ratio between the areas of $\Delta A'B'B$ and $\Delta BB'C'$ corresponds to the ratio of L_1 to L_2. Additionally, their *trisection lines* UU' and VV' respectively maintain distances of $L_1/3$ and $L_2/3$ from support B. Consequently, the x-coordinate of the vertical action line w of the resultant is also fixed and independent of the moment magnitudes. This fixed vertical line w is referred to as the *combined trisection line* (*verschränkte drittellinien*). It can be easily

[5]The ratio between its bending stiffness (EI) and length (L) is commonly referred to as "bending stiffness", "flexural stiffness/rigidity", or simply as "stiffness". The term "rotational stiffness" is chosen to distinguish this ratio from these more general terms.

[6]Mohr's Second Theorem: the linear deflection of an elastic curve at any given point, relative to the slope line projected from another point, multiplied by EI, equals to the moment of the area, about the first point, of the bending moment diagram between the two points (Mohr 1868).

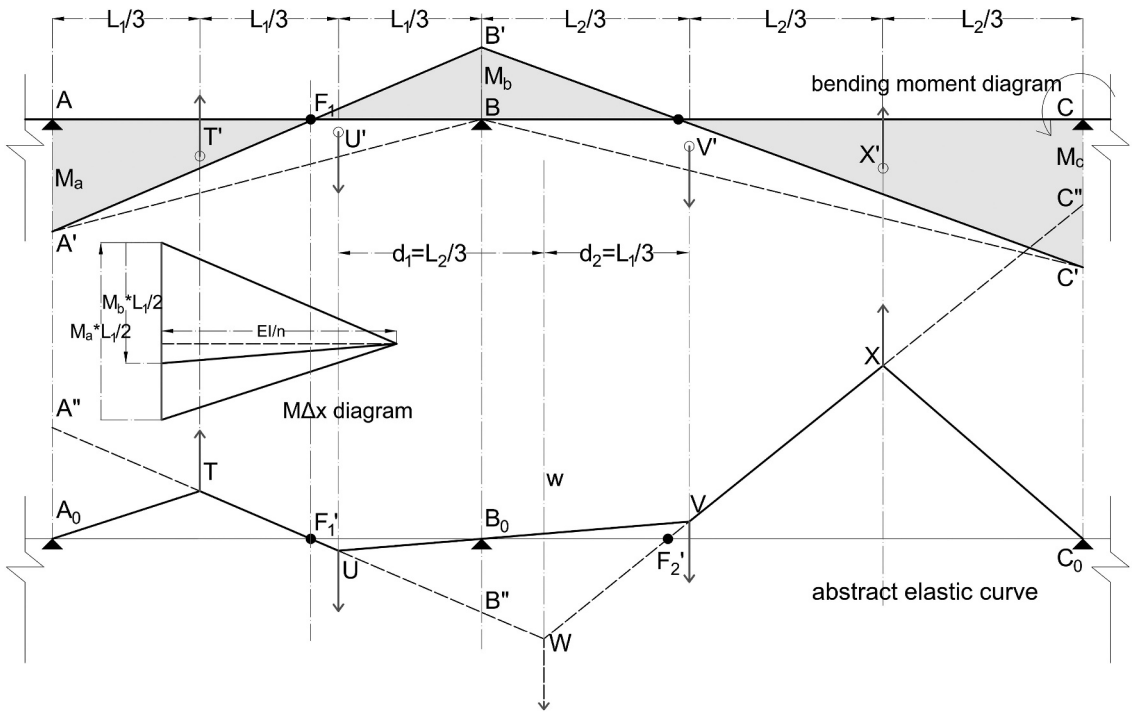

Figure 6. The continuous beam *ABC*, along with its bending moment diagram (hatched), *mδx diagram*, and the *abstract elastic curves*. For ease of representation, the ratio between support moments is distorted. Source: modified and redrawn from (Chalmers 1881).

proved that the distance between *w* and *UU'* is $L_2/3$, while that between *w* and *VV'* is $L_1/3$. The vertical *w* intersects the extension of *TU* at point *W*.

Then the second edge of the *abstract elastic curve VX* can be plotted by connecting *W* to *V* and extending it until it intersects *trisection line XX'* at *X*. This is due to the collinearity between *WV* and *VX*, resulting from the equilibrium of the funicular polygon *UWV*. As proved earlier, the x-intercept of *WV* coincides with the fixed point. The intersection between line *WV* and the baseline, denoted as F_2', denotes the fixed point. The last edge of the funicular polygon can be easily plotted by connecting point *X* to C_0. It is important to note that constructing the *abstract elastic curve* for span *BC* does not require the *MΔx diagram*.

4.4. The continuous beams with non-constant second moment of area

For continuous beams featuring an non-constant second moment of area, the process of determining fixed points generally remains unchanged, except for the action lines of the elastic weight.

If the second moment of area varies span-wise while remains constant within each span, the second moment of area must be involved in determining the *combined trisection line*. The distances from the *combined trisection line* to its two *trisection lines* are proportionate to the second moment of area of the member and inversely proportional to the length of the member. For example, assuming the second moment of area of the span *AB* (I_1) in Figure 6 is different from that of *BC* (I_2), the ratio of d_1 to d_2 should equal $\frac{I_1 L_2}{I_2 L_1}$.

In instances where the second moment of area varies within the span, the action lines are the resultants of the area of the diagram of *M/EI* instead of the moment diagram. Therefore, they no longer trisect the span, although are still independent of bending moment. Consider span *AB* in Figure 7, of which the member height increases near the right end *B*, resulting in an increased second moment of area. The action lines of the elastic weight due to the moment propagated from either side are graphically determined using the funicular polygon loaded by the area of the diagram of *M/EI* (hatched in oblique lines) instead of the triangular moment diagram (hatched in grey). Note that the action lines tend to approach the thinner end and no longer necessarily locate within one-third of the member length.

5. The fixed-points method for continuous beams

The process of constructing the bending moment diagram of a continuous beam using the *fixed-points*

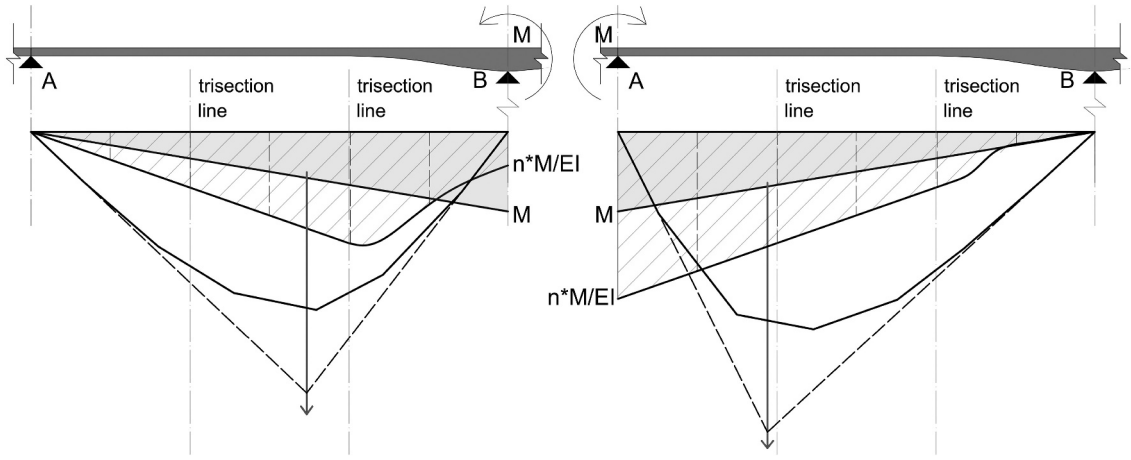

Figure 7. The action lines of the elastic weight due to the moment propagated from either side are determined with the diagram of *M/EI* (hatched in oblique lines). The bending moment diagram (hatched in light grey) and trisection lines are also drawn for comparison.

method is depicted in the flow chart presented in Figure 8. Initially, the fixed points are pinpointed based on the length and the second moment of area of each span. Then the bending moment diagram of a loaded span is obtained through the superposition of its closing string and the funicular polygon of the loading. The funicular polygon of the loading is plotted using a *force diagram*. The crossing lines, determining the closing string of the loaded span, are derived from the funicular polygon and the fixed points of the loaded span. Finally, the moment propagated to the unloaded spans is plotted using a train of straight lines. These lines connect the ends of the closing string of the loaded span to the fixed points of the unloaded span in a sequential manner. This sequential connection represents the propagation of moments through the structure.

5.1. Determining the fixed points of continuous beams

The *abstract elastic curve* of triangulated moment areas enables the consecutive determination of fixed points for continuous beams with any number of spans, without requiring knowledge of the actual moment. Consider the continuous beams $S_1S_2S_3S_4S_5$ in Figure 9(1) as an example, of which the second moments of area is constant. The first two spans bear evenly distributed loads, while the third span sustains a point load. The left and right series of fixed points are, respectively, denoted as F_n and I_n. The F_n series (solid points) in Figure 9(2) represents the fixed contraflexure points when an imaginary moment is exerted on S_5 and propagates leftward, while the I_n series (solid points) in Figure 9(3) signifies those for an imaginary moment imposed on S_1 and transmitted rightwards.

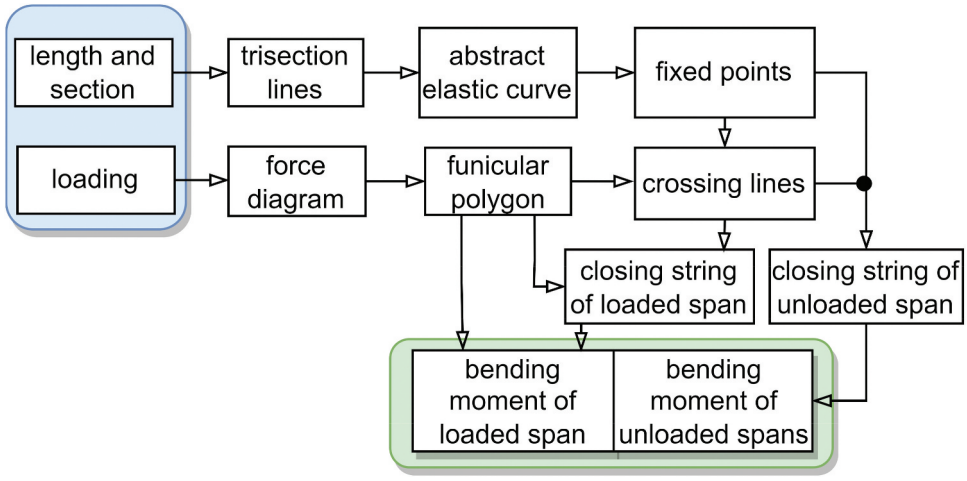

Figure 8. The procedure of analyzing continuous beams with the *fixed-points method*.

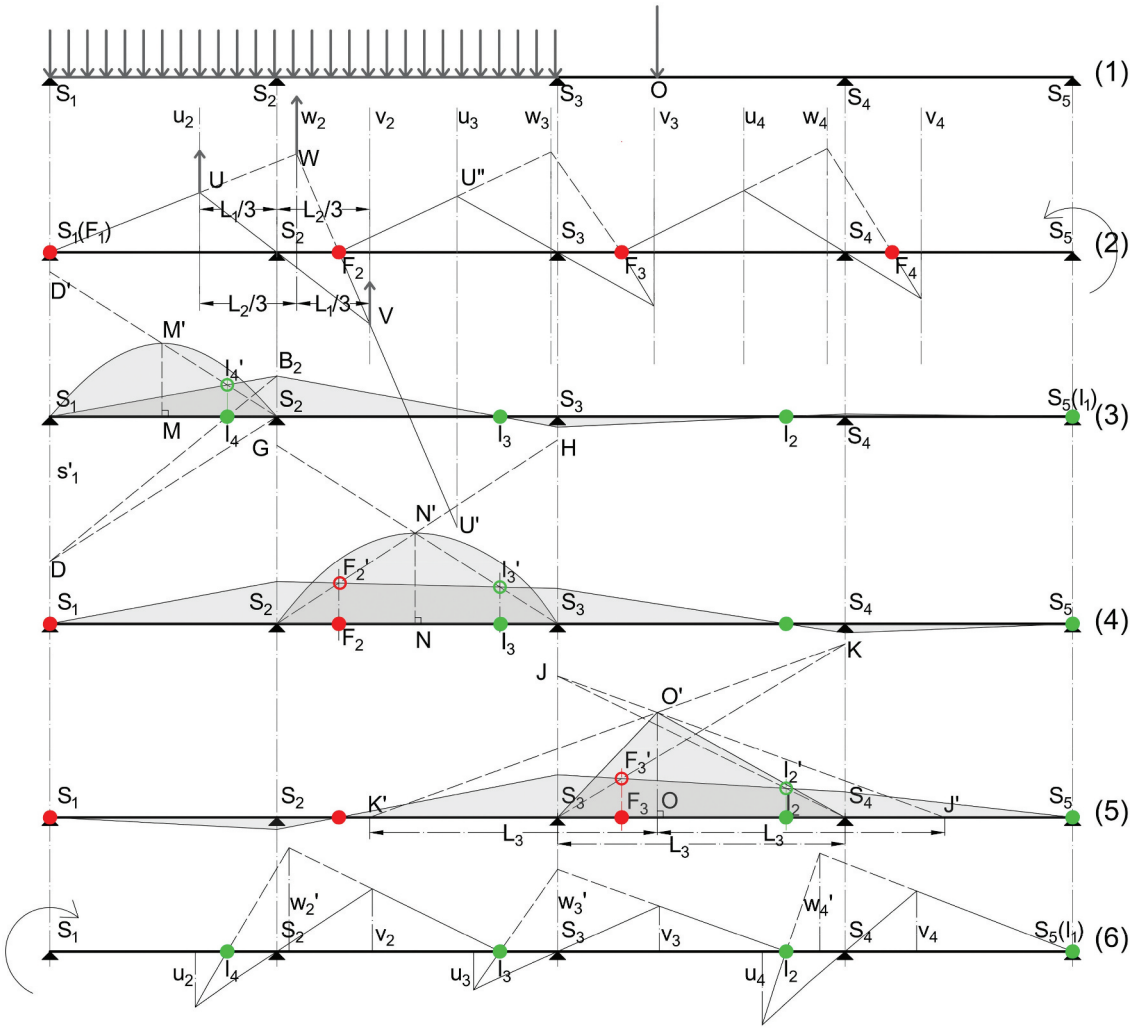

Figure 9. The analysis of a continuous beam with the *fixed-points method*.
(1) The continuous beam and its loads. (2) Determing the left fixed points with the *abstract elastic curves*. (3) Determining the moment induced by the load of the first span with a crossing line. (4) Determining the moment induced by the load of the second span with crossing lines. (5) Determining the moment induced by the load of the third span with crossing lines. (6) Determing the right fixed points with the abstract elastic curves. Source: Adapted and modified from (Mohr 1868).

The determining of the F_n series of fixed points begins from the leftmost point S_1, as illustrated in Figure 9(2). Initially, the first fixed point F_1 coincides with S_1, as the moment at the hinge support S_1 remains zero regardless of the moment imposed on S_5. To locate F_2, *trisection lines* u_2, v_2 and their *combined trisection line* w_2 are drawn. The first edge of the *abstract elastic curve* originates from point S_1 with an arbitrary slope, intersecting verticals u_2 and w_2 respectively at points U and W. Subsequently, the second edge, represented by line US_2, intersects vertical v_2 at point V. Then the subsequent edge VU' is drawn by connecting W and U and extending until intersecting the *trisection line* u_3 at U'. The intersection of line VU' and the x-axis pinpoints the fixed point (F_2) of the second span.

Since F_2 maintains zero bending moment regardless of the moment at S_5, it can be considered a freely rotatable end like S_1. Therefore, for ease of drawing, the construction of the *abstract elastic curves* proceeds with the line $F_2U"$, whose slope is arbitrary, in place of using F_2U'. The determination of fixed points F_3 and F_4 follows the same iterative process. The fixed points of the I series are then determined similarly, but from the terminal support S_5, as demonstrated in Figure 9(6).

5.2. Determining the bending moment induced at loaded span with the crossing lines

As illustrated in Figure 9(3–5), the bending moments induced by the loads in different spans are individually

determined using crossing lines. Subsequently, the resultant bending moment can be obtained by summing up the induced moments.

Let us consider the first loaded span S_1S_2, prior to determining the crossing lines, the positive moment of the load is depicted with the funicular polygon $S_1M'S_2$, with its vertex at point M'. The funicular polygon represents the statically determinate moment of the load and is plotted above the reference line. This moment induces the reactive negative statically indeterminate moment at continuous joint S_2 (represented by line B_2S_2), which propagates successively to the spans on the right. Both kinds of moments at this span are plotted above the reference line, despite their opposite signs. To determine the moment at S_2, first join S_2 and M' and extend until intersecting the vertical line s_1' at point D'. Line $D'S_2$ is the crossing line of this span, and it intersects the vertical of the predetermined fixed point I_4 at I_4'. The closing string S_1B_2 must pass through I_4', and thus is determined.[7]

For the intermediate span like S_2S_3, the closing string is located by two crossing lines, as illustrated in Figure 9(4). The lines GS_3 and HS_2 are plotted by connecting the supports to N', which is the vertex of the moment parabola of the statically determinate moment. The closing string at this span can be determined with the points F_2' and I_3', which are the intersections between the crossing lines and the verticals of fixed points. The demonstration can be readily derived from the one above.

For spans like S_3S_4 which is under a point load at point O, the crossing lines JS_4 and KS_3 no longer pass through the vertex of the moment diagram of load (point O'), as illustrated in Figure 9(5). To plot the crossing lines, first, points K' and J' are located on the baseline by measuring off the horizontal distance of the span L_3 from point O. Then the y-intercepts of crossing lines (points K and J) are obtained by projecting the height of vertex O' from point K' and J' to the verticals of supports on the opposite side. Then draw the crossing lines JS_4 and KS_3 and locate the closing string $F_3'I_2'$ with the same procedure.[8] This technique of crossing lines can also be applied to a span under multiple loads by graphically pre-determining their resultant with the technique in *subsection 3.1*.

6. The fixed-points method for continuous frames

6.1. One-story continuous frames without lateral displacement

As shown in Figure 10, within a continuous frame, the bending moment of the beam undergoes a discontinuity at the rigid joint due to the moment resistance of the columns. The presence of continuous T-joints poses two challenges when applying the *fixed-points method*. First, the *abstract elastic curve* used to pinpoint fixed points needs modification to consider the moment resistance of columns. Second, after determining the closing string at loaded spans, the moment needs to be distributed to two connected members via the T-joint based on their respective stiffness. Wilhelm Ritter introduced the "*E-line*" (*E-Linie*) and the *moment distribution angle* to address these two issues, respectively.

The "*E-line*" is a fixed vertical line that divides the distance between the *combined trisection line* and the *trisection line* of the second span in accordance with the stiffness of the columns and the previous beam. For instance, in Figure 10(3), the vertical line e is the *E-line* for determining the left fixed points of the second span. Vertical line e divides the distance between the *combined trisection line* w and *trisection*

[7]To comprehend the principle behind the crossing line, suppose the moment at S_2 is given (represented by the length of B_2S_2). Connect B_2 to the fixed point I_4 and extend the line until it intersects the vertical line s_1' at point D. Assume the removal of the load and the imposition of a positive moment at S_1, whose magnitude is represented by the length of line S_1D. According to the concept of the fixed point, this hypothetical moment would propagate through fixed point I_4, inducing a moment at S_2 whose magnitude is represented by the height of B_2S_2. Consequently, the angular deflection at support S_2 induced by this hypothetical moment is equivalent to that of the actual load of the first span. Therefore, the linear deflection at support S_1, relative to the slope line projected from S_2, both equals the slope at support S_2 multiplied by L_1. According to Mohr's Second Theorem, the moment of the moment area of the parabola $S_1M'S_2$ about point S_1 must equal that of the ΔS_1DS_2. Therefore, $\frac{1}{2}*S_1S_2*\frac{2}{3}*S_1S_2*M'M = \frac{1}{3}*S_1S_2*\frac{1}{2}*S_1S_2*S_1D$. We can deduce that: $S_1D = 2*M'M$.

The equation holds true regardless of the magnitude of the distributed load, and the entire derivation is reversible. Consequently, we can determine the length of B_2S_2 by measuring off twice the length of MM' downward from S_1 to D and projecting the length of S_1D via I_4 to the vertical of S_2. As the length of S_1D' is also double the height of $M'M$ and equals S_1D, the length of B_2S_2 can be more conveniently determined by projecting S_1D' via I_4' using the crossing line $M'S_2$.

[8]KS_4 is the height of the projection of vertex O' from point K' to the verticals of support S_4. Due to the similarity between $\Delta K'KS_4$ and $\Delta K'O'O$, KS_4 equals $\frac{(L_3+b)h}{L_3}$, in which L_3 is the span, b the length of OS_4, and h the length of OO'. Consequently, the moment of the area of triangle ΔKS_3S_4 about support S_3 equals $\frac{L_3(L_3+b)h}{6}$. This moment is the same as the moment of the area of triangle $\Delta O'S_3S_4$ about point S_3. According to Mohr's Second Theorem, the bending moment area of ΔKS_3S_4 and $\Delta O'S_3S_4$ would induce the same deflection at the spans on the left side of S_3. Similarly, ΔJS_3S_4 and $\Delta O'S_3S_4$ would induce the same deflection at the span on the right side of S_4 (Chalmers 1881, 215–218).

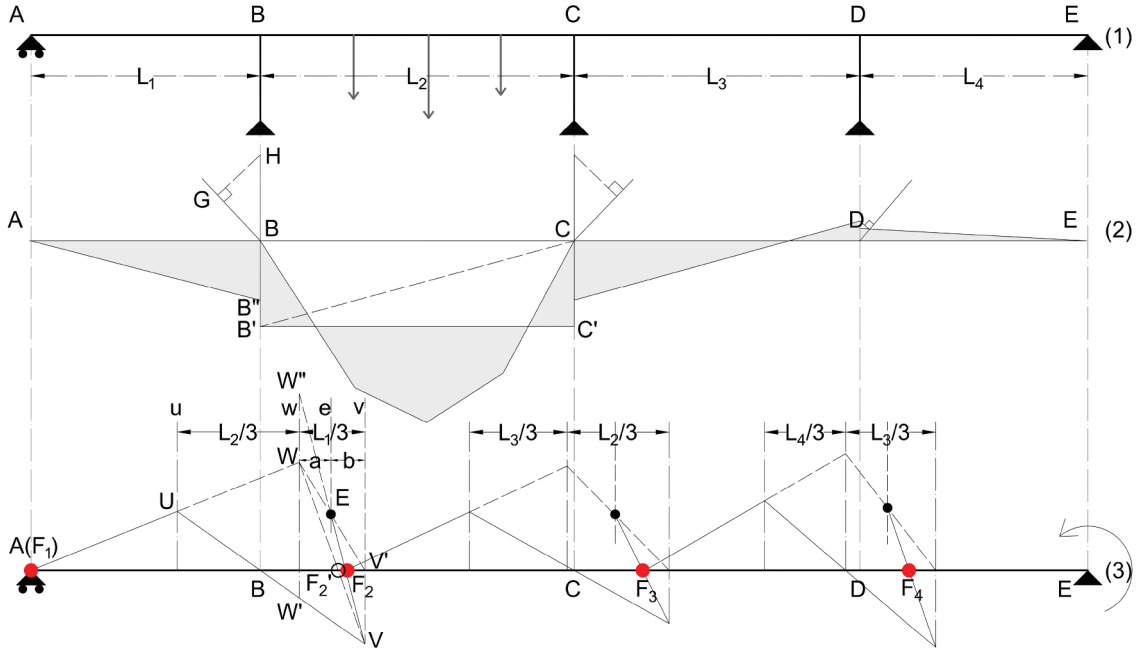

Figure 10. Analysis of a one-story continuous frame using the *fixed-points method*. (1) the frame and applied load. (2) the bending moment diagram and *moment distribution angles*. (3) determining fixed points (solid points) using the *abstract elastic curve* and *E-lines*. Source: adapted and modified from (Ritter and Culmann 1900, 130–131).

line v at the ratio of *a* to *b*, which is half the ratio of the end stiffness of the column head to the rotational stiffness of the beam.[9] The abscissa of *e* is independent of the bending moment, like the x-coordinates of *w* and *v*.

To determine the fixed points of the span *BC*, start by drawing the line *AU* from the first fixed point *A* at an arbitrary slope, intersecting *trisection line u* and *combined trisection line w* at points *U* and *W*. Then connect point *U* to support *B* and extend to intersect *trisection line v* at point *V*. Unlike the *abstract elastic curve* for continuous beams, the fixed point does not lie at F_2' (black circle), which is the x-intercept of line *WV*. Instead, connect points *W* and *V*', where *V'* is the intersection between vertical line *v* and the baseline. Point *E* (black point) is the intersection between line *WV'* and the vertical line *e*. Finally, the fixed point F_2 is determined by the intersection between *EV* and the baseline. The demonstration can be found in the reference (Ritter and Culmann 1900, 131). Following the same approach, the fixed points of subsequent spans are determined iteratively using predetermined *E-lines*. With the fixed points, the closing string *B'C'* of the loaded span *BC* is established using crossing lines.

Subsequently, the moment distributed to the adjoining unloaded spans *AB* and *CD* are determined graphically with the *moment distribution angles*, as depicted above the moment diagram in Figure 10(2). For example, *the moment distribution angle* for span *AB* is drawn above joint *B*, with its hypotenuse is on the extension of *B'B*. The other side of the angle (*GB*) is plotted by setting the sine of the angle *HBG* equal to the ratio of the end stiffness[10] of *AB* to the combined end stiffness *AB* and the left column. The length of *BB'* is measured off upward from point *B*, reaching point *H*. Consequently, the moment carried by span *AB* can be measured from is the distance from point *H* to line *GB*. This distance is measured off downward from point *B* to located *B"*. Thus, the bending moment diagram of *AB* is plotted by joining *A* to *B"*, and the moment carried by the columns head is represented by the length of *B'B"*. This graphical method is efficient when dealing with moments distributed from

[9]The length *W'W"* is the relative deflection induced by the elastic weight of the moment area of $\triangle BB'C$ at the vertical *w*. According to Mohr's second theorem and the explanation in 3.2, $W'W = \frac{n}{EI} \cdot A_{BB'C} \cdot \frac{1}{3}L_1$. In this equation *n* is the scale factor for the abstract elastic curve (all the y-coordinates is *n* times the corresponding actual deflection), $\frac{1}{3}L_1$ is the distance between the triangle centroid and the vertical *w*, $A_{BB'C}$ is the area of $\triangle BB'C$ and equals $\frac{1}{2} \cdot BB' \cdot L_2$. Likewise, $W'W = \frac{n}{EI} \cdot A_{ABB} \cdot \frac{1}{3}L_2$, in which $A_{BB'C}$ equals $\frac{1}{2} \cdot BB \cdot L_1$. It follows $WW = W'W - W'W = \frac{n}{6EI} \cdot L_1 \cdot L_2 \cdot B'B$

Meanwhile, the end stiffness of the column head is denoted as ε, the rotation at joint *B* as τ, which equals $\frac{B'B}{\varepsilon}$. The slope of line *UV* is *n* times τ. As point *V'* trisects the span, $VV' = n \cdot \tau \cdot \frac{1}{3}L_2 = \frac{n}{3\varepsilon} \cdot B'B \cdot L_2$.

Finally, due to the similarity between $\Delta EWW''$ and $\Delta EV'V$, $a : b = WW : VV' = \frac{1}{2}\left(\varepsilon : \frac{EI}{L_1}\right)$

[10]Like in the moment distribution method (Cross 1932), the end stiffness of a structural member is the moment that need to be applied to an end of the member to induce a unit rotation of that end. it equals $\frac{3EI}{L}$ for members pinned at the other end like *AB*, *CD* and columns, $\frac{4EI}{L}$ for members fixed at the other end, in which *L* is the length of the member in question. For members rigidly connectedly to other member(s) at other end, like the member *BC*, its end stiffness can be numerically determined with the *rotation angle method*.

multiple loaded spans, which will be exemplified by the Weissensteinstrasse Overpass in *subsection 7.2*.

6.2. Continuous frames with lateral displacement

Continuous frames would undergo horizontal displacement due to lateral loading at beam-column joint. Besides, the lateral displacement can also be caused by factors such as unsymmetrical vertical loading, unsymmetrical form, and different columns supports. The horizontal displacement can induce significant moments in the columns, necessitating analysis with caution. This subsection will explain the analysis of one-story continuous frames using the *fixed-points method*. This method has also been adapted for multi-story frames (Suter and Traub 1951, 67–74). However, akin to the *moment distribution method*, its application becomes cumbersome for such problems.

The analysis of a one-story continuous frame lateral loaded at its beam-column joint is similar to that of a continuous beam. The difference lies in the generation of moments, which occurs through deflected columns instead of loaded beams. The generated moment is then propagated through the fixed points of other members and summed up. However, as the portion of the lateral loading carried by each column is currently unknown, the moment cannot be directly computed from the load. To determine the moment induced at columns, initially, the actual load F is replaced by an unknown virtual load f which can induce a unit virtual lateral displacement at the beam. We then calculate the moment generated by this unit displacement at each column. Subsequently, we determine the magnitude of the virtual load f by summing up the propagated moment. By scaling the total moment induced by force f at the ratio of F to f, we can obtain the actual moment of the frame under the lateral point load F.

If the lateral displacement is induced by the above-mentioned factors other than lateral point load, a virtual lateral constraint is imposed at the beam-column joint to retain the frame in place (Figure 11). This allowed the analysis of this retained frame using Ritter's method to determine both the moment and the retaining force R imposed by this constraint. Subsequently, the moment induced by lateral displacement can be quantified by applying the counterforce of R as the point load on the frame. Finally, the internal forces of the original frame were determined by combining the internal forces of these two decomposed systems.

7. Robert Maillart's application in the analysis of bridge frames

During his studies at ETH Zurich, Robert Maillart (1872–1940) learnt graphic statics during lectures with Wilhelm Ritter. He adeptly applied graphic statics in his exploration of innovative and efficient structural forms (Fivet and Zastavni 2012; Zastavni 2008). Maillart employed the *fixed-points method* in at least two reinforced concrete bridges: the bridge over the Simme river in Garstatt (German: Brücke über die Simme in Garstatt, 1939–40) and the Weissensteinstrasse Overpass (German: Überführung der Weissensteinstrasse, 1938). The application of this method in these two bridges is evidenced by their documented static calculations, which stated that the calculation was according to the book of (Suter, Baumann, and Häusler 1932). Despite being later, the application on the Garstatt Bridge is presented first due to its more rudimentary nature.

The Garstatt Bridge over the Simme was designed in 1940 and is in the small village of Garstatt in the Canton of Bern, Switzerland. The structure primarily comprises two parallel three-hinged arches, each of which is composed of twin box girders. Additionally, beyond each arch, the load of the bridge deck is further supported by the continuous L-frame (Figure 12).

Due to the great stiffness of the box girder, the left support of the beam which was embedded into the box girder was modelled as a rigid support. The column base of the L-frame was also embedded into the solid foundation, resulting in a three-degree static indeterminacy. Disregarding enlargement of the beam section at the

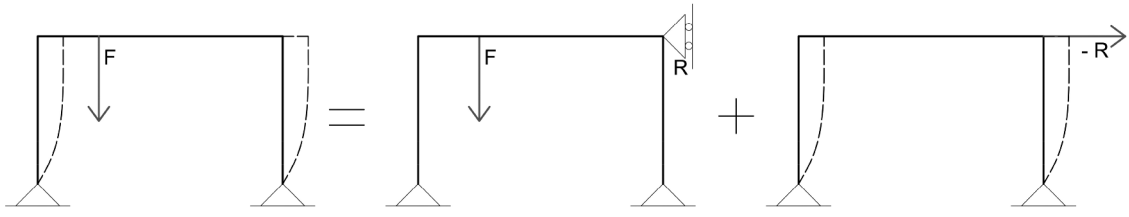

Figure 11. The analysis of a portal frame that undergoes laterally displacement due to unsymmetrical vertical load. The structure system is decomposed into a laterally constrained frame and a frame solely loaded by the counterforce of the retaining force.

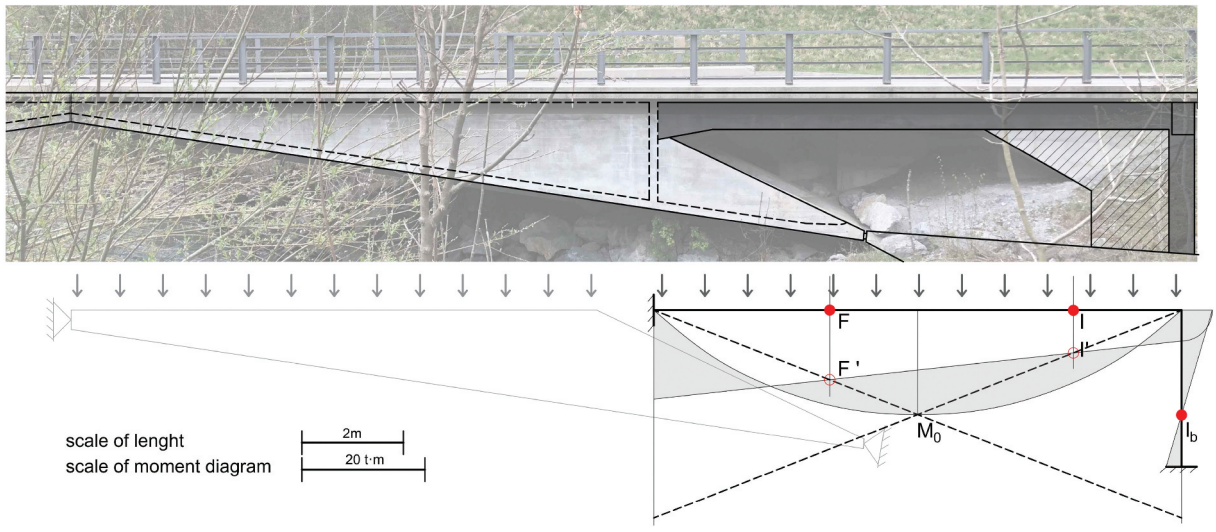

Figure 12. Top: the L-frame (solid grey hatching) and the box girder of the Garstatt Bridge, with the recently added panel (hatched in oblique lines). Source: plotted on a photo photographed by the authors in 2022. Bottom: Maillart's analysis of the L-frame. Source: modified from the original drawing.

Figure 13. Views of the Weissensteinstrasse Overpass from the west and below. Source: photographed by the authors in 2022.

ends, Maillart assumed the second moment of area of the L-frame to be constant.

7.1. The L-frame of the Garstatt Bridge over the simme river

The analysis process of this L-frame is similar to that of a two-span continuous beam which is subjected to uniformly distributed load at the left span. Initially, the fixed points of the beam (F and I) and the lower fixed point of the column (I_b) were located. Since the frame is clamped at both supports, the fixed points F and I_b are situated at the trisection point of their member. The location of the right fixed point (I) was derived from rotational stiffness of the two members using the *rotation angle method*. Meanwhile, the funicular polygon of the statically determinate moment of the distributed vertical load was readily plotted. With the maximum value of the moment (M_0) of load and fixed points F and I, the closing string $F'I'$ was determined using crossing lines. The end moment at joint B is propagated to the column, whose diagram is determined by drawing a line passing through fixed point I_b. Finally, the reactions at the supports and shear force were deduced from the bending moment.

7.2. The three-span continuous frame of the weissensteinstrasse overpass

The Weissensteinstrasse Overpass is an auto road bridge designed and erected in 1938. It is located near the Fischermätteli station in Bern, Switzerland. The deck is supported by twin continuous frames which span over railways (Figure 13). Each of the twin continuous frames is embedded at column bases E and F and supported by rollers at ends A and D (Figure 14), resulting in eight freedom constraints and a total of five degrees of external static indeterminacy. The girder height increases towards the continuous joints, correlating with the increase of the bending moment of vertical loading. Thanks to its simplicity yet structurally effectiveness, this bridge was praised as one of Maillart's finest works (Bill 1955, 132).

As explained in 3.3, the bending moment diagram of each loaded span comprises a funicular polygon, which

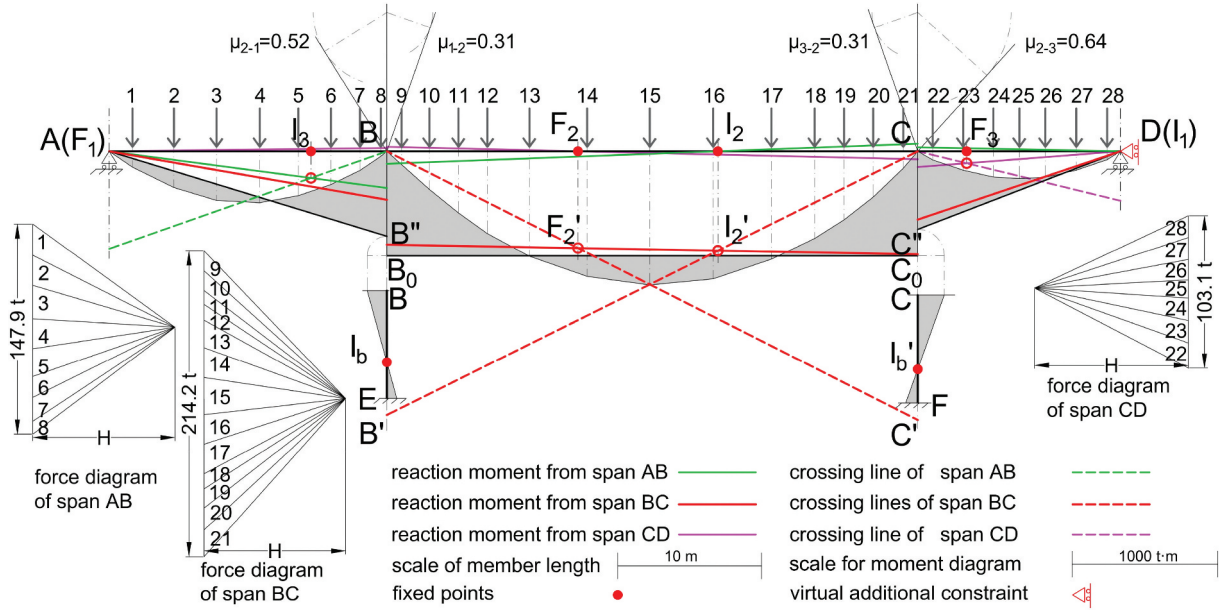

Figure 14. The analysis of the weissensteinstrasse overpass with the *fixed-points method*. Source: redrawn from the original drawing.

represents the statically determinate moment of the load, and a closing string. The closing string represents the statically indeterminate bending moment induced by the "joining force" at continuous joints. The ordinate of the closing string of a span equals the sum of the statically indeterminate bending moment of the span considered and the propagation of such bending moment in other spans. Taking the bending moment diagram of span *BC* (hatched area in Figure 14) as an example, it is defined by the funicular polygon joining *BC* and the closing string B_0C_0. The ordinate of closing string B_0C_0 is the summation of the hyperstatic bending moment from span *BC* (red line *B"C"*) and the bending moments distributed from the hyperstatic bending moments in spans *AB* (green solid line) and *CD* (magenta solid line).

To construct the bending moment diagram, firstly, the funicular polygon for the statically determinate moment of load was constructed using *force diagrams* with the method briefed in 3.1 (Figure 14). Take span *BC* for example, the vertical loading of the middle span *BC* was divided into segments represented by discrete point loads *9–21* which are placed at the center of mass of each of these divisions. The divisions closer to the joints with vertical legs were denser due to the increased dead load modeling thicker beam sections. These point loads were then transposed onto the load line in the corresponding *force diagram*, based on which the funicular polygon of load moment was constructed below the baseline.

Subsequently, the preliminary closing string for the hyperstatic bending moment at *B"C"* was determined using *fixed points* F_2 and I_2, along with the crossing lines *BC'* and *CB'*. The *fixed points* were located numerically by employing the *rotation angle method*, which considered the varying second moment of area. The distribution factors of members *AB* and *CD* were deduced from their rotational stiffness and both equal 0.31. The magnitude of the bending moment propagated from *BC* to these spans was determined graphically using the *moment distribution angles* above joints *B* and *C*.

Similarly, the statically indeterminate bending moments induced on side spans *AB* and *CD* were individually determined with crossing lines and then propagated to the other spans of the girder. It is important to note that the statically indeterminate bending moment from span *AB* propagated via the right fixed point I_2, whereas that of span *CD* propagated via left fixed point F_2. The hyperstatic bending moments of these three spans and their propagation were combined to obtain the total hyperstatic bending moment of the girders. The bending moment at the top of the column equalled the difference between bending moments of the ends of two girders connected to it. The oblique lines for the bending moment diagrams of the columns were then constructed through the *fixed points* of the columns. As depicted in Figure 14, the overall bending moment was represented by the shaded area which is enclosed by the closing strings and the funicular polygons[11]

[11]Given its asymmetrical beam spans, this frame would undergo lateral displacement under the vertical load. To evaluate the effect of the lateral displacement, a virtual lateral constraint was added to support *D* (red roller support in Figure 14). The moment induced by lateral displacement equals that by the counterforce of the retaining force imposed by the virtual constraint. This moment was determined with the procedure explained in 6.2. However, the resulting moment was found to be negligible.

8. Discussion and conclusion

Through historical research and a detailed technical presentation of dedicated solving methods and their applications, this article demonstrates that graphic statics can be and has been used to analyze statically indeterminate structures of continuous beams and continuous frames. The evolution of the *fixed-points method* is reviewed in relation to its historical background, offering insights into both its development and decline. Additionally, the principles and procedures of the *fixed-points method* are briefly introduced. This technical knowledge lays the ground for an explanation of Robert Maillart's utilization of the *fixed-points method* in designing two bridges.

8.1. Contributions

This article presents the most comprehensive survey of the history of the *fixed-points method*, to the best of the authors' knowledge. Section 2 complements existing knowledge of the history of graphic statics. Despite being unduly neglected, the *fixed-points method* occupies a significant place in the history of structural theory. It represents a crucial yet imperfect attempt to extend graphic statics to address emerging practical challenges in the development of structures. Its definitive abandonment contributed significantly to the decline of graphic statics.

This paper also extends the comprehension of Maillart's design approach for continuous-structure bridges, a topic that has been relatively overlooked and partly misunderstood. Moreover, there are reasons to conjecture that some of Maillart's other bridges, which have long been associated with continuous beams, may also have been designed as a continuous frame.

This technical explanation of the *fixed-points method* has the potential to benefit historical research into the works of other engineers, as this method appears to have been popular then.

9. Limitations, discussion, and future work

This review of the *fixed-points method* is far from complete. Other works may have contributed to this method and deserve to be investigated. Additionally, it remains unclear whether the *fixed-points method* was used to refine structural forms rather than solely as an analysis tool for predetermined forms. The examination of Maillart's design methods on other works, such as the Salginatobel Bridge and the Chiasso Shed, revealed that Maillart employed commonly utilized analysis techniques not just for analytical purposes but also to refine the structural geometries (Fivet and Zastavni 2012; Zastavni 2008). Furthermore, during the investigation of historical writings, we uncovered other graphical methods for continuous beams and frames. An upcoming paper dedicated solely to these methods is currently in preparation.

Beyond historical research and heritage preservation, a question of greater practical significance arises: can an extension of *fixed-points method* finds relevance in contemporary structural teaching and design, akin to the graphical methods for reticular structures?

On one hand, the graphical version of the *fixed-points method* is less mathematically demanding and aligns with the graphical thinking patterns commonly employed by architects. As a result, it bears the potential to serve as an accessible common platform facilitating communication between architects and structural engineers. Moreover, the assurance of static equilibrium, conveyed through the geometric interplay among diagrams, allows for dynamic adjustments in both geometry and bending behavior. This two-way approach, historically utilized and currently revived for pin-jointed structures, not only yields visually captivating designs but also ensures structural efficiency (D'acunto et al. 2019; Fivet and Zastavni 2012). Additionally, the fixed point, central to this method, visually elucidates the correlation between member stiffness and bending moment. Designers using the *fixed-points method* can thus make informed decisions regarding modifying member sections. This cognitive value for design was confidently underscored in the preface of (Suter, Baumann, and Häusler 1932, V):

> If a truly artistic architecture is to develop once again, it can only come from people who know exactly how the forces flow within the structural elements and who are able to design the outer forms in accordance with this. However, there is hardly a better way to familiarize yourself with the internal course of forces in complicated architectural structures than to work using the *fixed-points method.*

On the other hand, due to the intricate nature of continuous structures, the relations presented by the *fixed-points method* are not as readily accessible as those of pin-jointed structures by conventional graphic statics. Besides, this graphical method is somewhat complicated in terms of the ease of comprehending and learning. The complex principles and procedures hinder its potential in both dissemination and application as a design tool. The somewhat abstruse *abstract elastic curve* not only obscures the relation between stiffness and moment but also obstructs the possible bi-directional design approach.

For these reasons, improvements are necessary to realize the promising potential of the *fixed-points method* as a practical design tool. One possible direction is to simplify the method by merging it with approximate methods like the portal or cantilever method. Another approach is computerization and parameterization, revolutionizing the efficiency of graphical methods by automating some mathematical process while maintaining the visual dimension of the method. In addition, previous studies (Muttoni, Schwartz, and Thürlimann 1996; Rondeaux and Zastavni 2018) have demonstrated that graphic statics applies perfectly to plastic analysis, showing its great efficiency for structural design. Yet the full potential of the *fixed-points method* for plastic design of continuous beams and frames remains to be ascertained.

Acknowledgments

The authors would also like to acknowledge the ETHZ for granting access to Maillart's original working drawings.

Disclosure statement

No potential conflict of interest was reported by the author(s).

Funding

This research is funded by China Scholarship Council (CSC, No. 201706190234) and the supporting grants from UCLouvain.

References

Allen, E., and W. Zalewski. 2009. *Form and forces: Designing efficient, expressive structures*. Hoboken, New Jersey & Canada: John Wiley & Sons.

Bill, M. 1955. *Robert Maillart*. 2d ed. Zürich: Girsberger.

Billington, D. P. 1979. *Robert Maillart's bridges: The art of engineering*. Reprinted edition. Princeton, N.J: Princeton University Press.

Block, P., and L. Lachauer. 2014. Three-dimensional (3D) equilibrium analysis of gothic masonry vaults. *International Journal of Architectural Heritage* 8 (3):312–35.

Boothby, T. E. 2015. Engineering iron and Stone: Understanding structural analysis and design methods of the Late 19th Century.

Capecchi, D. 2012. Historical roots of the rule of composition of forces. *Meccanica* 47 (8):1887–901.

Chalmers, J. B. 1881. *Graphical determination of forces in engineering structures*. London: Macmillan & Co.

Charlton, T. M. 1982. *A history of theory of structures in the nineteenth century*. Cambridge, London, New York, New Rochelle, Melbourne, Sydney: Cambridge University Press.

Costa-Jover, A., J. Lluis i Ginovart, and S. Coll-Pla. 2017. Limit analysis and the study of building stages in masonry structures. Experiences with the gothic apse of tortosa cathedral (1345–1441). *International Journal of Architectural Heritage* 11 (4):475–89.

Cross, H. 1932. Analysis of continuous frames by distributing fixed-end moments. *Transactions of the American Society of Civil Engineers* 96 (1):1–10.

Culmann, C. 1866. *Die graphische Statik*. 1st ed. Zürich: Verlag von Meyer und Zeller.

Culmann, C. 1875. *Die graphische Statik*. Vol. 1, 2nd ed. Zürich: Verlag Von Meyer und Zeller.

Cusano, C., A. Montanino, C. Cennamo, G. Zuccaro, and M. Angelillo. 2023. Geometry and stability of a double-shell dome in four building phases: The case study of Santa Maria Alla Sanità in Naples. *International Journal of Architectural Heritage* 17 (2):362–88.

D'acunto, P., J.-P. Jasienski, P. Ole Ohlbrock, C. Fivet, J. Schwartz, and D. Zastavni. 2019. Vector-based 3D graphic statics: A framework for the design of spatial structures based on the relation between form and forces. *International Journal of Solids and Structures* 167:58–70.

Du Bois, A. J. 1875. *The elements of graphical statics and their application to framed structures*. New York: John Wiley and Son.

ETH-Archiv. 2018. Biographisches Dossier Ernst Suter (1884-) von Basel; PD für Methode der Festpunkte an der ETH. https://eth.swisscovery.slsp.ch/permalink/41SLSP_ETH/lshl64/alma99117435336605503.

Fang, D. L., R. K. Napolitano, T. L. Michiels, and S. M. Adriaenssens. 2019. Assessing the stability of unreinforced masonry arches and vaults: A comparison of analytical and numerical strategies. *International Journal of Architectural Heritage* 13 (5):648–662. doi:10.1080/15583058.2018.1463413.

Fivet, C., and D. Zastavni. 2012. Robert Maillart's key methods from the salginatobel bridge design process (1928). *Journal of the International Association for Shell and Spatial Structures* 53 (1):39–47.

Fivet, C., and D. Zastavni. 2015. A fully geometric approach for interactive constraint-based structural equilibrium design. *Computer-Aided Design* 61:42–57.

Guldan, R. 1943. *Rahmentragwerke und Durchlaufträger*. 2nd ed. Vienna: Springer-Verlag Wien GmbH.

Han, S., and D. Zastavni. 2022. A historical graphical analysis method for rigid frames. IASS/APCS 2022 Beijing Symposium: Next Generation Parametric Design, Beijing, China, September 19-22. https://www.ingentaconnect.com/contentone/iass/piass/2022/00002022/00000008/art00025.

Han S., and D. Zastavni. 2023. Fixed-Points Method in Robert Maillart's Analysis of Rigid Frame Bridges. In *the International Conference on Structural Analysis of Historical Constructions (SAHC 2023)*, Kyoto, eds. Y. Endo and T. Hanazato, 68–77. Cham: Springer. doi:10.1007/978-3-031-39603-8_6.

Hartz, C., M. M. Arek Mazurek, T. M. Tomás Zegard, and W. F. Baker. 2018. The application of 2D and 3D graphic statics in design. *Journal of the International Association for Shell and Spatial Structures* 59 (4):235–42.

Henn. 1951. Ernst Suter, Die Methode der Festpunkte. *ZAMM - Journal of Applied Mathematics and Mechanics/Zeitschrift für*

Angewandte Mathematik und Mechanik 31 (8–9):299. doi:10.1002/zamm.19510310862

Hirschfeld, K. 1959. Berechnung statisch unbestimmter systeme. In *Baustatik: theorie und beispiele*, ed. K. Hirschfeld, 171–684. Berlin: Springer. doi:10.1007/978-3-662-30166-1_5.

Huerta, S. 2006. Structural design in the work of Gaudi. *Architectural Science Review* 49 (4):324–39.

Karanikoloudis, G., P. B. Lourenço, L. E. Alejo, and N. Mendes. 2021. Lessons from structural analysis of a great gothic cathedral: Canterbury cathedral as a case study. *International Journal of Architectural Heritage* 15 (12):1765–94.

Kavanaugh, C., I. Mae Morris, R. Napolitano, and J. Jose Jorquera-Lucerga. 2017. Validating the use of graphical thrust line analysis for pier buttresses: The case study of amiens cathedral. *International Journal of Architectural Heritage* 11 (6):859–70.

Koechlin, M. 1889. *Applications de la statique graphique*. Vol. 1. Paris: Baudry et C^{ie}, libraires-éditeurs.

Kurrer, K.-E. 2018. *The history of the theory of structures: Searching for equilibrium*. Berlin: John Wiley & Sons.

Levy, M. M. 1886. *La statique graphique et ses applications aux constructions*, Vol. 2, 2nd ed. Paris: Gauthier-Villars.

Mohr, C. O. 1868. Beitrag zur theorie der holz-und eisenkonstruktionen. *Zeitschrift des Architekten- und Ingenieurvereins zu Hannover* 14 (19–51):397–400.

Müller-Breslau, H. F. B. 1892. *Die graphische Statik der Baukonstruktionen* 2. vollständig umgearbeitete und wesentlich vermehrte Aufl. ed. Vol. 2.Leipzig: Baumgärtner's Buchhandlung.

Muttoni, A., J. Schwartz, and B. Thürlimann. 1996. *Design of concrete structures with stress fields*. Basel, Boston, Berlin: Birkhauser.

Navier, C. L. M. H. 1833. *Resume des lecons sur l' application de la mecanique. . .ect*. Paris: NP.

Pillet, J. 1895. *Traité de stabilité des constructions : Leçons professées au Conservatoire national des arts et métiers et a l'Ecole spéciale d'architecture, Cours techniques de l'architecte et du constructeur*. Paris: En vente au dépot des cours techniques.

Ramos, L. F., and T. Sturm. 2014. Seismic safety analysis of the old Portuguese cathedral in Safi, Morocco. *International Journal of Architectural Heritage* 8 (4):475–97.

Rankine, W. J. M., and V. L. Roberts. 1858. *A manual of applied mechanics*. 1st. ed. *Encyclopaedia Metropolitana; or, System of Universal Knowledge: on a methodical plan/ projected by Samuel Taylor Coleridge* London: R. Griffin.

Ritter, K. W. 1871. *Die elastische Linie und ihre Anwendung auf den kontinierlichen Balken: ein Beitrag zur graphischen Statik*. Zürich: Meyer und Zeller.

Ritter, W. 1883. *Die elastische linie und ihre anwendung auf den continuirlichen balken: Ein beitrag zur graphischen statik. Mit 12 textfiguren und 1 lithographirten tafel*. Zürich: Meyer & Zeller (H. Reimmann).

Ritter, W., and K. Culmann. 1900. *Anwendungen der graphischen Statik. Dritter Teil. Der Kontinuierliche Balken 4 vols*. Vol. 3. Zurich: Meyer & Zeller.

Robin, R. C. 1933. A graphical solution of statcally indetermiant frames. *Journal of the Institution of Engineers, Australia* 5 (No. 5):145–60.

Rondeaux, J.-F., and D. Zastavni. 2018. A fully graphical approach for limit state analysis of existing structures: Application to plane elastic-plastic bended structures and to plane masonry arches. *International Journal of Architectural Heritage* 12 (3):409–31.

Saliklis, E. 2019. *Structures: A geometric approach*. Cham, Switzerland: Springer.

Sattler, K. 1969. Statisch unbestimmte Systeme. Festpunktmethode. In *Lehrbuch der Statik: Theorie und ihre Anwendungen. Erster Band: Grundlagen und fundamentale Berechnungsverfahren*, ed. K. Sattler, 357–87. Berlin, Heidelberg: Springer Berlin Heidelberg.

Suter, E. 1916. *Berechnung des kontinuierlichen Balkens mit veränderlichem Trägheitsmoment auf elastisch drehbaren Pfeilern sowie Berechnung des mehrfachen Rahmens mit geradem Balken nach der Methode der Fixpunkte*. Berlin: Springer.

Suter, E. 1923. *Die Methode der Festpunkte*. 1st ed. Berlin: Springer-Verlag.

Suter, E., O. Baumann, and F. Häusler. 1932. *Die Methode der Festpunkte zur Berechnung der statisch unbestimmten Konstruktionen mit zahlreichen Beispielen aus der Praxis insbesondere ausgeführten Eisenbetontragwerken*. Berlin: Springer-Verlag.

Suter, E., and E. Traub. 1951. *Die Methode der Festpunkte*. 3 ed. Berlin/Göttingen/Heidelberg: Springer Berlin, Heidelberg.

Varignon, P. 1725. *Nouvelle mecanique ou statique: dont le projet fut donné en MDCLXXXVII* Vol. 2. chez Claude Jombert.

Wolfe, W. S. 1921. *Graphical analysis; a text book on graphic statics*. 1st ed. New York, etc.: McGraw-Hill book company, inc.

Zastavni, D. 2008. The structural design of Maillart's chiasso shed (1924): A graphic procedure. *Structural Engineering International* 18 (3):247–52.